Peak Shape Analysis and Plate Theory for Plasma Chromatography

Glenn E. Spangler and Charles I. Collins

U.S. Army Mobility Equipment Research & Development Center, Fort Belvoir, Va. 22060

The peak shape in plasma chromatography is proportional to the difference between two error functions whose arguments differ by $V_d t_g / 2\sqrt{D_L t_d}$. When $V_d t_g \ll 2\sqrt{D_L t_d}$, the peak shape reduces to a Gaussian and under conditions where large ion concentrations become involved, corrections must be made for electrostatic repulsion. The *HETP* is

$$\text{HETP} = \frac{4l_d}{5.54(2l_d + \mu E t_g^2)} \left(\frac{11.090\eta KT l_d}{eE} + \mu^2 E^2 t_g^2 \right)$$

whose minimum corresponds to an optimum electrostatic drift field lying within a factor of 1.4 of the value obtained if the diffusion width is equated to the gate width. *HETP* values are less than those generally encountered in gas chromatography and mass resolution is less than those generally obtained in mass spectrometry.

Plasma chromatography has been developed during the past several years to detect, characterize, and analyze trace vapor constituents in gaseous mixtures at atmospheric pressure. The instrumentation utilizes a ^{63}Ni radioactive beta source to generate ions for reaction with the trace vapor to form characteristic positive and negative ion–molecule complexes. The complexes formed in the reaction region are separated in a coupled ion mobility-drift tube spectrometer and appear as a recorded ion mobility spectrum of separated ion–molecule peaks. Basic features of the method and the instrumentation are described elsewhere (1–3).

As pointed out by McDaniel (4), drift tube spectrometry, and therefore plasma chromatography, is capable of measuring the transport properties and reactions of slow ions in gases. When appropriate precautions are taken, drift velocities, diffusion coefficients, reaction rates, and equilibrium constants for the ions can be determined through arrival-time spectra and ionic current levels. Measurements can be made as a function of gas temperature, drift field, gas composition, and total pressure. On the other hand, plasma chromatography is also capable of providing much the same information as gas chromatography in nearly real time and at sensitivities characteristic of the electron capture detector. Quantitative data are obtained only when the ion–molecule reactions are determined and controlled. Since much of the information required to perform satisfactory plasma chromatography is contained in the shape of the ion peak, this study was undertaken to derive a theory capable of describing the peak shape and to compare it with experimental results. The Cl$^-$ ion obtained from the injection of o-dichlorobenzene into the instrument was used as the diagnostic ion (5).

EXPERIMENTAL

Instrumentation. The data were collected on a Franklin GNO Beta VII Plasma Chromatograph operated in the one grid pulsing mode and equipped with a Nicolet 1024 signal averager for readout. The conversion factor for the preamplifiers preceding the sig-

nal averager was 5×10^9 V/A, and the trigger was the positive slope of the gate 1 pulse provided externally on the Beta VII instrument. Time constants for the system were 20 microseconds for the signal averager and 35 microseconds for the electrometer. The instrument temperatures were 198 °C for the inlet, 166 °C for the drift tube housing, and 182 °C for the carrier gas. The drift temperature was 160.3 °C as determined by a AWG 24 copper constantan thermocouple attached to a L&N 194 numatron and placed in contact with the drift space guard rings through the exit port of the drift tube. The drift gas was prepurified nitrogen as supplied by Airco flowing at a rate of 377 cm^3/min and the carrier gas was zero air as supplied by Matheson flowing at a rate of 44.5 cm^3/min. The drift field was constant at 214 V/cm with the cell pressure varying ambiently between $755 < P < 780$ mm Hg.

Procedure. The sample was prepared by adsorbing vapors from the vapor head space of a reagent grade supply of o-dichlorobenzene and desorbing the vapors into the heated inlet of the instrument. The quantity of vapor was sufficient to saturate the response of the instrument for a time period long compared to that required to collect data. A saturated response was felt necessary to eliminate electrostatic repulsion effects which could arise due to the presence of reactant ions in the drift region and to provide a constant signal for analysis. The Cl$^-$ ion appeared at the nominal drift time ($t_d + t_g/2$; $t_g = 0.05$ msec) of 7.92 msec independently of whether zero air or nitrogen was used in the reaction region. Data scanning the width of the Cl$^-$ peak were collected with the digital readout option of the signal averager as a function of the gate 1 pulse width setting. Corrections for base line and adjustments of the results to equivalent gain settings were made before reporting.

RESULTS AND DISCUSSION

Longitudinal Diffusion. The transport equation describing the three-dimensional drift and diffusion of a singly converting ion species in a drift tube is commonly taken to be

$$\frac{\partial n_1}{\partial t} = \mathfrak{D} n_1(\vec{x}) + S(\vec{x}) \tag{1}$$

where $n_1(\vec{x})$ is the local number density of ions, $S(\vec{x})$ is a source term and $\mathfrak{D}$ is an operator defined as

$$\mathfrak{D} \equiv D_T \left(\frac{\partial^2}{\partial x^2} + \frac{\partial^2}{\partial y^2} \right) + D_L \frac{\partial^2}{\partial z^2} - V_d \frac{\partial}{\partial z} + \langle \alpha \rangle - k_1^- \tag{2}$$

D_T and D_L are the transverse and longitudinal diffusion coefficients respectively, V_d is the drift velocity chosen to lie in the $+z$ direction, $\langle \alpha \rangle$ is the reaction frequency describing the conversion of other ions to n_1 ions, and k_1^- is the annihilation rate for the n_1 ions. Since these equations are derived from the equation of continuity and a first order approximation for the ion current density, they are valid only for low values of E/N or E/P where $mJ/P_{av} \ll \rho$ (6, 7). E is the electrostatic field, N is the number density of neutral gas atoms corresponding to a density ρ in the drift region, m and P_{av} are the mass and average momentum for the diffusing ions, and J is the diffusion flux rate. Both the conditions on E/N and mJ/P_{av} are satisfied in plasma chromatography when the system is operated under atmospheric pressure conditions.

Since Equation 1 is linear in n_1 and is similar in form to the Smoluchowski equation (8), it is amenable to standard kinetic theory treatment. For time intervals large com-
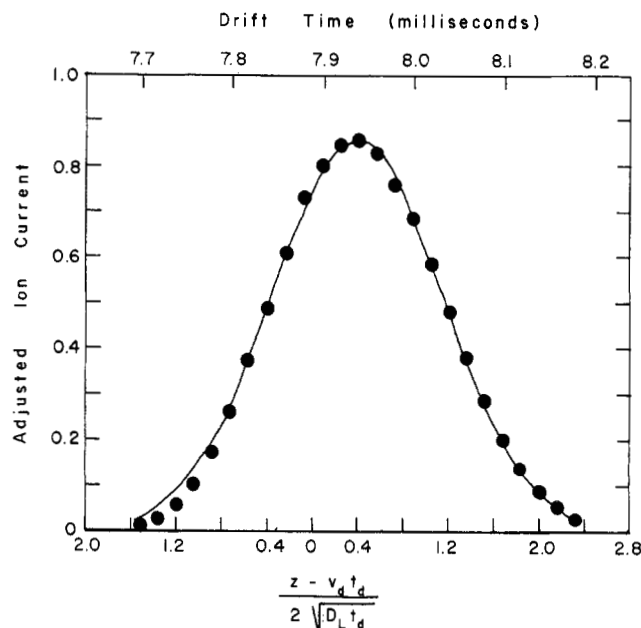
Figure 1. Comparison of theory (solid line) with experiment (dots) on the shape of the Cl⁻ ion peak in plasma chromatography

Experimental data were taken with an 0.10-msec gate width setting

pared to relaxation times in Brownian motion, Green function techniques can be applied where (9)

$$G(\vec{x}) = \frac{1}{[(4\pi D_T t)^2 4\pi D_L t]^{1/2}} \exp[(\langle\alpha\rangle - k_1^-)t] \times$$

$$\exp\left[-\frac{x^2 + y^2}{4D_T t} - \frac{(z - V_d t)^2}{4D_L t}\right] \quad (3)$$

and

$$n_1(\vec{x}) = \int d^4x' G(\vec{x} - \vec{x}') S(\vec{x'}) \quad (4)$$

The time integration runs from $-\infty$ to t and the space integration runs from $-\infty$ to $+\infty$.

Various authors (7, 9–11) have solved Equation 4 for various assumed functional forms of $S(\vec{x}')$, but the most appropriate for plasma chromatography is a rectangular pulse of width $V_d t_g$ where t_g is the gate 1 pulse width. This type of source term is described mathematically by the Heaviside step function H so that

$$S(r', \theta', z', t') = f(r')[H(z') - H(z' - V_d t_g)]\delta(t') \quad (5)$$

where r' is the radial coordinate in cylindrical geometry. Assuming that $f(r)$ is constant at an assumed value of n_0 and that effects due to walls are negligible, equations 3–5 become

$$n_1(r, \theta, z, t) = \frac{n_0 \exp[(\langle\alpha\rangle - k_1^-)t]}{4\pi^{3/2} t D_T} \int_0^{r_0} r' dr' \int_0^{2\pi} d\theta'$$

$$\int_{\frac{(z - V_d t - V_d t_g)}{2\sqrt{D_L t}}}^{\frac{(z - V_d t)}{2\sqrt{D_L t}}} \exp\left\{-\frac{r^2 + r'^2 - 2rr' \cos(\theta - \theta')}{4D_T t}\right\} \times$$

$$\exp(-\xi^2)d\xi \quad (6)$$

where $\xi = (z - z' - V_d t)/2\sqrt{D_L t}$. Utilizing the definition of the error function (12) and the solution supplied by McDaniel *et al.* (13) for the remaining integrals, a simplified expression for the ion concentration on axis at $r = 0$ is
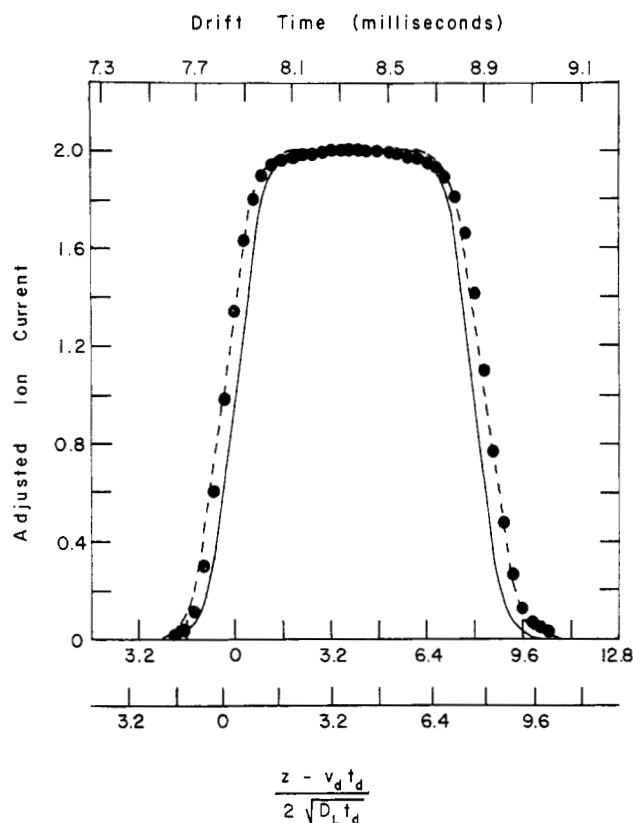
Figure 2. Comparison of theory (solid and broken lines) with experiment (dots) on the shape of the Cl⁻ ion peak in plasma chromatography

Experimental data were taken with an 1.0-msec gate width setting and the theoretical curves are for vapor diffusion (solid line) and vapor diffusion corrected for electrostatic repulsion (broken lines), respectively

$$n_1(o, z, t) = \frac{n_0}{2} \exp[(\langle\alpha\rangle - k_1^-)t] \times$$

$$\left[1 - \exp\left(-\frac{r_0^2}{4D_T t}\right)\right] \times \left[\text{erf}\left(\frac{z - V_d t}{2\sqrt{D_L t}}\right) - \right.$$

$$\left. \text{erf}\left(\frac{z - V_d t - V_d t_g}{2\sqrt{D_L t}}\right)\right] \quad (7)$$

A more complete expression for the radial dependence of $n_1(\vec{x})$ can be obtained from reference *13*. Since the aperture grid of the Beta VII plasma chromatograph has a diameter of 3.18 cm, r_0 is 1.59 cm and $r_0^2/4D_L t_d \gg 1$ where t_d is the mean drift time. This allows effects related to translational diffusion to be neglected.

The ionic current flux is related to the ionic number density through

$$J_1(o, z, t) = -D_L \frac{\partial n_1}{\partial z} + V_d n_1 \quad (8)$$

so that for the conditions $V_d t_g > 4\sqrt{D_L t}$ and $V_d (\pi t/D_L)^{1/2} \gg 1$ satisfied in plasma chromatography,

$$J_1(o, z, t) \simeq \frac{n_0 V_d \exp[(\langle\alpha\rangle - k_1^-)t]}{2} \times$$

$$\left[\text{erf}\left(\frac{z - V_d t}{2\sqrt{D_L t}}\right) - \text{erf}\left(\frac{z - V_d t - V_d t_g}{2\sqrt{D_L t}}\right)\right] \quad (9)$$

The error functions of Equation 9 are plotted in Figures 1 and 2 as a function of $z/2\sqrt{D_L t_d}$ which has been chosen as the independent variable to eliminate the necessity to correct for t in the denominator. Experimental data as a function of t are also plotted which have been adjusted to

Table I. Comparison of Theory with Experiment Regarding the Effect of Molecular Diffusion on Peak Shape

Gate width, t_g, msec	Peak maximum $\mathrm{erf}\left(\dfrac{v_d t_g}{2\sqrt{D_L t_d}}\right)$	Experimental (arb. units)	Peak width $\omega_{1/2}$, msec	Experimental, msec	HETP Theoretical (cm $\times$ 10^4)	Experimental (cm $\times$ 10^4)
0.05	0.23	0.14	0.21	0.20	10.10	9.20
0.10	0.43	0.41	0.23	0.22	11.76	11.10
0.20	0.74	0.76	0.29	0.27	18.42	16.53
0.50	1.00	1.00	0.54	0.57	63.49	71.51
1.00	1.00	1.12	1.02	1.09	212.0	245.5

match the curves at the peak maximum. Data and theory match best when $V_d/2\sqrt{D_L t_d}$ is 8.2×10^3 sec^{-1}. Peak maxima occur at $t_d + t_g/2$ with t_d equal to 7.88 msec corresponding to a reduced mobility of 2.99 cm^2 volt^{-1} sec^{-1}. This mobility differs by less than 3% from 2.92 cm^2 volt^{-1} sec^{-1} previously reported for the Cl$^-$ ion (14, 15) when the drift tube housing temperature was used as the drift region temperature. The amplitude of the peak maximum is proportional to erf $(V_d t_g/4\sqrt{D_L t_d})$ which is recorded in Table I for $V_d/2\sqrt{D_L t_d}$ = 8.2×10^3 sec^{-1}. Also recorded are experimental data adjusted to agree with the theoretical value obtained for $t_g = 0.50$ msec. The large discrepancy which exists between experiment and theory for the 0.05-msec gate width setting is probably related to the distorted waveform for the gate pulse used on this setting. For ($\langle \alpha \rangle$ − k_1^-) = 0, the instrument calibration suggests that the data adjustment corresponds to an ion number density of 1.64×10^6 ions/cm^3 in the reaction region.

For $V_d t_g/2\sqrt{D_L t_d}$ small, Equation 9 reduces to a Gaussian with a standard deviation σ_Z of $\sqrt{2D_L t_d}$. Since $z = V_d t$, the standard deviation σ_t for t is $\sqrt{2D_L t_d}/V_d$ if $\sigma_{V_d} \simeq \sigma_{z \times V_d}$ = 0. The peak width at half maximum under these conditions is

$$\lim_{\frac{V_d t_g}{2\sqrt{D_L t_d}} \to 0} \omega_{1/2} = \frac{4\sqrt{\ln(2)\, D_L t_d}}{V_d} \tag{10}$$

independent of the gate width. For $V_d t_g/2\sqrt{D_L t_d}$ large, $\omega_{1/2}$ satisfies

$$\lim_{\frac{V_d t_g}{2\sqrt{D_L t_d}} \to \infty} \omega_{1/2} = t_g \tag{11}$$

Thus an appropriate expression for the peak width at half maximum is

$$\omega_{1/2} = \sqrt{\frac{11.090\, D_L t_d}{V_d^2} + t_g^2} \tag{12}$$

This is recorded in Table I for $V_d/2\sqrt{D_L t_g}$ = 8.2×10^3 sec^{-1} along with experimentally observed values. It is noted that a gate 1 pulse width of 0.20 millisecond is a good compromise between a loss in resolution resulting from excessively broad peaks obtained at large gate widths and a loss in sensitivity which accompanies reduced amplitudes at shorter gate widths.

Mutual Repulsion. As observed in Figure 2, the diffusion model lacks a complete description for the shape of the ion peak. The reason is that corrections must be made for electrostatic repulsion between the ions as they drift through the drift region. If the ion peak is assumed to be a slab of ions of finite width but of infinite radial extension, Gauss's law in electrostatics can be applied to calculate the change in the electric field which develops in the slab due to the presence of the ions. The result is (16)
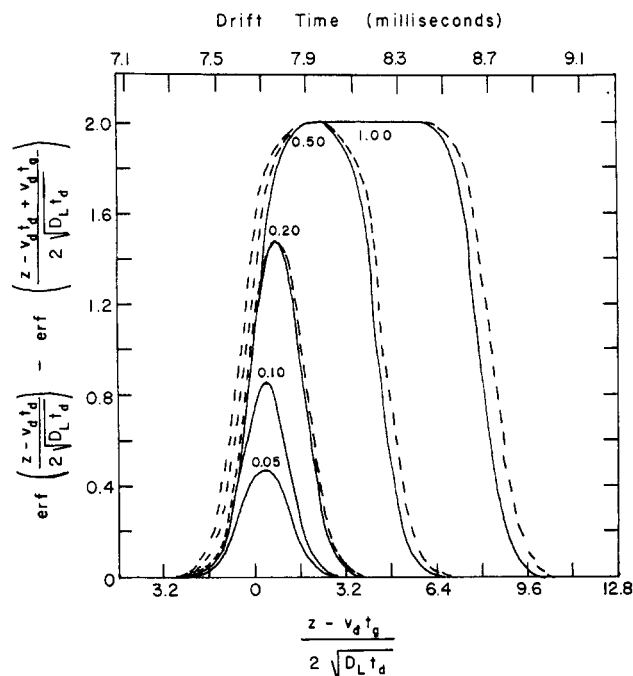
Figure 3. Summary of the predictions of Equation 9 (solid lines) on the shape of the Cl$^-$ ion peak as a function of gate width setting.

The broken lines are the corrections for electrostatic repulsion necessary to make theory agree with experiment

$$\Delta \vec{E} = \frac{n_0 \vec{V}_d (t - t_d - t_g/2)}{2\epsilon}; \quad t_d < t < t_d + t_g \tag{13}$$

Consequently, the velocity of the leading edge of the pulse exceeds that of the trailing edge by

$$\Delta \vec{V}_d = \mu \Delta \vec{E} = \frac{n_0 \mu^2 \vec{E} t_g}{2\epsilon} \tag{14}$$

where μ is the mobility. When corrections for this are made to the diffusion theory, the broken curve of Figure 2 is obtained. The curve fits much better the experimental results. The size of the correction is such that an ion concentration n_0 of 5.26×10^7 ions/cm^3 is required to account for the additional spreading. This is an order of magnitude greater than that estimated from the peak amplitude data but can be accounted for by allowing $\langle \alpha \rangle$ of Equation 9 to be equal to zero and k_1^- to be equal to 440 sec^{-1}. For a cell temperature of 433 °K, this value of k_1^- corresponds to an annihilation rate constant of 2.59×10^{-17} cm^3 sec^{-1}. Since the drift field cannot be varied independently in the drift and reaction regions of the Beta VII instrument without modification, this annihilation rate was not verified more directly experimentally (15). Values based on considerations of electrostatic repulsion may be off by several orders of magnitude. Figure 3 is a summary of the predictions of Equation 9 along with corrections in accordance with Equation 13.

Table II. Parameters Affecting Peak Shape in Gas Chromatography and Plasma Chromatography

	Gas chromatography	Plasma chromatography
Separation	Proportional to partition coefficient (Retention time)	Proportional to ionic mobility (Drift time)
Peak broadening	Diffusion in gas (mobile) phase Resistance to mass transfer in liquid phase	Diffusion in drift gas
Parameters affecting *HETP*	Column temperature Carrier gas pressure Carrier gas flow rate Liquid phase type and loading Retention time or column length Tortuosity of column packing Mesh of solid support material	Drift tube temperature Drift gas pressure Drift field Drift gas composition Drift time or drift length Mobility
Corrections to peak broadening or *HETP*	Injection profile Decomposition Solute reactions in column Dead volume Response time of detector Adsorption isotherms	Gate 1 pulse shape Ion stability and/or clustering Ion–molecule reactions in drift region Electrostatic repulsion Response time of current measuring/ readout device

Plate Theory and Resolution. Although great differences exist between gas chromatography, plasma chromatography, and mass spectrometry, certain analogies can be drawn between the three technologies concerning the optimization of sensitivity and resolution. Resolution with a 10% valley is well defined for mass spectrometry and the number of theoretical plates describes column efficiency in gas chromatography. Similar considerations will now be given to plasma chromatography.

The number N of theoretical plates in gas chromatography is borrowed from distillation and is related to the ratio of the square of the mean adjusted retention volume V_R to the variance σ_V^2 or the square of the mean adjusted retention time t_R to the variance σ_t^2 (17). The variance is related to the peak width at half maximum through $\omega_{1/2}^2 = 5.54\,\sigma^2$. In an analogous manner, the number of theoretical plates in plasma chromatography can be defined as

$$N = 5.54 \left(\frac{t_d + t_g/2}{\omega_{1/2}} \right)^2 \tag{15}$$

where the retention time becomes the drift time. If the drift length l_d in plasma chromatography corresponds to the column length in gas chromatography, the HETP ("height equivalent to a theoretical plate") also becomes

$$\text{HETP} = \frac{l_d}{N} \tag{16}$$

Equations 12, 15, and 16 suggest

$$\text{HETP} = \frac{4l_d}{5.54(2l_d + \mu E t_g)^2} \left(\frac{11.09\eta K T l_d}{eE} + \mu^2 E^2 t_g^2 \right) \tag{17}$$

where a modified expression for the Einstein relation (18)

$$\frac{\mu}{D_L} = \frac{e}{\eta K T} \tag{18}$$

has been used to simplify the expression. η is the Townsend energy factor which equals the ratio of the mean agitation energy of the ion to the mean thermal energy of the molecules in the drift region and is a monotonically increasing function of E/p. For the experiments described on the Cl⁻

ion, η equals 2.7. In the limit as t_g goes to zero or l_d goes to infinity, the HETP becomes

$$\text{limit}_{\substack{t_g \to 0 \\ l_d \to \infty}} \text{HETP} = \frac{2\eta K T}{eE} \tag{19}$$

which is equivalent to twice the diffusion coefficient over the drift velocity (18). Equation 19 states that the limiting HETP is directly proportional to the characteristic agitation energy for the ions and inversely proportional to the drift field.

Displayed in Table I are the calculated values of the HETP as derived from Equation 17 where $\eta = 2.7$ and $V_d/2\sqrt{D_L t_g} = 8.2 \times 10^3$ sec⁻¹. Also recorded are the HETP values observed experimentally. For the 0.05-msec gate width setting, the values approach the theoretical limit of 9.58×10^{-4} cm as calculated from Equation 19. The discrepancies at larger gate widths are a result of peak broadening due to electrostatic repulsion. Corrections for electrostatic repulsion are not included in the calculated HETP values.

Mass resolution in mass spectrometry is defined as $M/\Delta M$ where ΔM is the mass separation resolved when a 10% valley exists between two ion peaks. If, in plasma chromatography, the ion drift time is assumed to obey the empirical relationship (19)

$$\log_{10} t_{dl} = \frac{4}{9} \log_{10} M + 0.157 \tag{20}$$

where M is the molecular weight, t_{dl} is the drift time at 472 °K in milliseconds, and the drift length is 8 cm, then

$$\frac{t_{dl}}{\Delta t_{dl}} = -\frac{\mu}{\Delta \mu} = \frac{9}{4} \frac{M}{\Delta M} \tag{21}$$

If the shape of the ion peaks is a Gaussian, the 10% valley (twice 5% of the maximum amplitude) appears at 2.45 σ and t_{dl} is 2.09 $\omega_{1/2}$. Under these conditions, mass resolution for plasma chromatography is

$$\frac{M}{\Delta M} = \frac{t_d + t_g/2}{4.7 \, \omega_{1/2}} \tag{22}$$

where the more correct expression for the drift time, $t_d + t_g/2$, is used instead of t_{dl}. Theoretically, $M/\Delta M$ cannot be better than 8.3 for the Cl^- ion data being reported. When the gate width contributes to peak broadening, Equation 22 becomes

$$\frac{M}{\Delta M} = (t_d + t_g/2)\left(\frac{48.4\,D_L t_d}{V_d^2} + t_g^2\right)^{-1/2} \quad (23)$$

CONCLUSION

A theory has been developed to describe the peak shape of ion peaks in plasma chromatography. For short gate widths, the peak shape is essentially Gaussian with the width at half maximum being proportional to the square root of the drift time and inversely proportional to the drift velocity. Spreading due to electrostatic repulsion is observed at larger gate widths with the degree of spreading being directly proportional to the drift time and gate width. Efficiency of chromatographic analysis is achieved by adjusting the electrostatic field and gate width so that their product minimizes the *HETP*. For a given gate width t_g, the *HETP* is minimized when the electrostatic drift field obeys

$$E_{opt} \simeq \left(\frac{11.09\,\eta KT l_d}{2e\mu^2 t_g^2}\right) \quad (24)$$

Thus for $T = 433\ ^\circ K$, $l_d = 8$ cm, $\eta = 2.7$, $\mu = 4.74$ cm^2 volt^{-1} sec^{-1}, and $t_g = 0.10$ msec, E_{opt} is 271 volt/cm. Within a factor of 1.4, Equation 24 is approximated by $(4D_L t_d)^{1/2} = V_d t_g$ where the diffusion width equals the gate width. Since field strengths in excess of 251 volts/cm break down the carrier gas at 433 $^\circ K$, there is no theoretical advantage in going to shorter gate widths than 0.10 msec. Even in using the 0.10-msec gate width setting, reduced electrostatic drift fields are needed to prevent gas breakdown. The 0.10-msec gate width settings are preferred to 0.20-msec gate width settings so that space charge effects can be minimized. On the other hand, space charge effects on small signals well separated from the reactant ion peaks are negligible.

Karasek, Laub, and deDecker (20) have reported computerized deconvolution of peak data in plasma chromatography. From their data, the peak widths at half maximum were approximately 0.20 msec for Cl^- and 0.147 msec for Br^-. Since these are greater than the 0.1-msec injection pulse width used in the experiments, Gaussian fits for the data appear justified. The width at half maximum for the deconvoluted peaks, however, are approximately 0.17 msec for $^{35}Cl^-$, 0.13 msec for $^{37}Cl^-$, 0.106 msec for $^{79}Br^-$, and 0.12 msec for $^{81}Br^-$. It is not understood why the deconvoluted peak width for $^{79}Br^-$ should be so close to the injection pulse width nor why the deconvoluted peak widths for the $^{35}Cl^-$, $^{37}Cl^-$, and $^{79}Br^-$ isotopes should decrease with increasing drift time. This contradicts the statement of Equation 10.

As a result, certain analogies and comparisons can be made between gas chromatography, plasma chromatography, and mass spectrometry even though widely varying technologies are represented. Summarized in Table II are the various parameters which affect peak shape in plasma chromatography and gas chromatography. Every attempt has been made to pair parameters having the same effect on the peak shape even though direct comparisons sometimes become difficult. Table II should not be taken as evidence that the two technologies are similar, since comparisons are being made on the basis of peak shape only. *HETP* values for plasma chromatography are several orders of magnitude below that for gas chromatography but this is primarily due to the short drift length utilized in plasma chromatography. A mass resolution of 8 is available in plasma chromatography as compared to 400 to 70,000 in mass spectrometry.

Finally, the effect of the shape of the injection gate pulse shape on the final peak shape must be emphasized. Discrepancies as a result of this appear in the data recorded in Table I. The peak shape obtained for the 0.05-msec gate width setting was greatly distorted and that obtained for the 0.10-msec gate width setting (see Figure 1) was affected at shorter drift times. A possible recommendation for improvement is to sharpen up on the leading edge of the gate 1 pulse so that data can be taken in a region where Gaussian spreading is known to be the only contributing factor.

LITERATURE CITED

(1) F. W. Karasek, *Res./Develop.*, 21 (3), 34 (1970).
(2) M. J. Cohen and F. W. Karasek, *J. Chromatogr. Sci.*, 8, 330 (1970).
(3) F. W. Karasek, *Res./Develop.*, 21 (12), 25 (1970).
(4) E. W. McDaniel, *J. Chem. Phys.*, 52, 3931 (1970).
(5) F. W. Karasek and O. S. Tatone, *Anal. Chem.*, 44, 1758 (1972).
(6) T. V. Vorburger, S. B. Woo, and J. H. Whealton, *J. Appl. Phys.*, 44, 2571 (1973).
(7) P. M. Morse and H. Feshbach, "Methods of Theoretical Physics," McGraw-Hill, New York, N.Y., 1953, Chap. 2.
(8) S. Chandrasekhar, *Rev. Mod. Phys.*, 15, 1 (1943).
(9) I. R. Gatland, "Ion Swarm Analysis," Technical Report, Georgia Institute of Technology, Atlanta, Ga., June 1972 (unpublished), copies available from author.
(10) J. H. Schummers, G. M. Thomson, D. R. James, I. R. Gatland, and E. W. McDaniel, *Phys. Rev.*, 7A, 683 (1973).
(11) S. B. Woo and J. H. Shealton, *Phys. Rev.*, 180, 314 (1969).
(12) M. Abramowitz and I. A. Stegun, "Handbook of Mathematical Functions," Dover, New York, N.Y., 1965, p 297.
(13) E. W. McDaniel, V. Cermak, A. Dalgarno, E. E. Ferguson, and L. Friedman, "Ion Molecule Reactions," Wiley-Interscience, New York, N.Y., 1970, pp 85–91.
(14) F. W. Karasek, O. S. Tatone, and D. M. Kane, *Anal. Chem.*, 45, 1210 (1973).
(15) G. E. Spangler and C. I. Collins, *Anal. Chem.*, 47, 393 (1975).
(16) S. T. Fisher, Final Technical Report No. LWL-CR-03C72A, Prepared by the Franklin Institute Research Laboratories, Philadelphia, Pa., for the U.S. Army Land Warfare Laboratory, APG, Md., August 1972.
(17) A. B. Littlewood, "Gas Chromatography," Academic Press, New York, N.Y. 1970, Chap. 5.
(18) E. W. McDaniel, "Collision Phenomena in Ionized Gases," Wiley, New York, N.Y., 1964, Chap. 10.
(19) S. P. Cram and S. N. Chesler, *J. Chromatogr. Sci.*, 11, 391 (1973).
(20) F. W. Karasek, R. J. Laub, and E. deDecker, *J. Chromatogr.* 93, 123 (1974).